Imaging defects in strained-silicon thin films by glancing-incidence x-ray topography

D. R. Black[a] and J. C. Woicik
National Institute of Standards and Technology, Gaithersburg, Maryland 20899

M. Erdtmann and T. A. Langdo
AmberWave Systems Corp., Salem, New Hampshire 03079

(Received 31 August 2005; accepted 4 May 2006; published online 2 June 2006)

X-ray topographical images from thin ($\leqslant$50 nm) strained-Si films grown on relaxed, planarized crystalline SiGe-on-Si (001) virtual substrates have been imaged by glancing-incidence monochromatic x-ray topography. This extremely asymmetric diffraction geometry, utilizing (311) diffraction planes, can limit penetration into the sample to as little as 6 nm and allows separate images from the thin strained-Si film, the SiGe layer, and the base Si wafer to be recorded at different angles above the critical angle. Strain fields from the misfit dislocations in the SiGe layer penetrate the Si wafer and act as a template for the defect structure of the strained-Si films, even after an *ex situ* planarization step was inserted during the growth of the SiGe layer. This defect structure remains in the strained-Si film throughout the fabrication of strained-Si-on-insulator substrates. © *2006 American Institute of Physics*. [DOI: 10.1063/1.2209411]

A method being developed to increase carrier mobility of silicon transistors is to introduce a small strain into the silicon lattice.[1] A biaxial tensile strain of 0.8% can increase the carrier mobility in Si by 80%,[2] leading to a significant improvement in device performance. This strain may be introduced by epitaxial deposition of a thin silicon film on a substrate with a slightly larger lattice parameter. Typically this "virtual substrate" is a relaxed, planarized crystalline SiGe alloy grown on a Si wafer, i.e., a fully relaxed $Si_{1-x}Ge_x$ graded buffer and constant-composition cap layer where x is between 0.1 and 0.5. The thickness of the thin silicon film is chosen to be less than the critical thickness for the expected strain[3] and is typically in the range of 10–50 nm. A critical aspect of this process is the control of defects in the SiGe layer and their propagation into the strained-Si film.

The defect structure of a well-controlled SiGe graded buffer layer grown on a Si (001) wafer is a set of 60° dislocations consisting of edge, tilt, and screw components. It is the inhomogeneous strain fields from the edge components (misfit segments) along the equivalent $\langle 110 \rangle$ directions that result in the characteristic crosshatch patterns observed experimentally.[4] X-ray topography (XRT) is a premier, nondestructive technique to study such defects in crystals.[5–7] In this letter, we describe research carried out at the NIST Materials Science and Engineering Laboratory x-ray topography station on beamline 33-BM at the Advanced Photon Source. This methodology is used to image defects in SiGe layers and to study how these defects affect both the strained-Si film and underlying Si wafer, and we have imaged these defects over the entire area of large-scale 8 in. production wafers.

A significant challenge for imaging defects in thin films is to have sufficient diffracted intensity, lateral resolution, and depth resolution to differentiate between diffractions arising from the thin film and the substrate. For example, without an analyzer crystal, the (004) diffraction from the Si wafer overwhelms the (004) diffraction from the strained-Si film, due to both limited angular resolution and inelastic scattering. To overcome these obstacles we utilize a (311) grazing-incidence x-ray diffraction geometry, Fig. 1, with the incident x-ray energy chosen so that the thin-film diffraction condition is satisfied at an incident angle just above the critical angle θ_c for total-external reflection, $\theta_c \sim 0.2°$ at 8.9 keV. In our various images, the diffraction condition is controlled by the selection of incident energy and angle so that we can selectively image the strained-Si film, the SiGe layers, and the Si wafer utilizing both our depth sensitivity and Q resolution. This highly asymmetric geometry increases the effective thickness of the film about 200 times; for reference the extinction length for the 113 diffraction is about 4 μm at 8.9 keV. When combined with the reciprocal-space resolution of our monochromatic x-rays, it enables the microstructure of the epitaxial strained film to be imaged that would otherwise not be visible. The relationship between the defect structure within the film and the underlying substrate layers may therefore be studied. The microstructure of relaxed SiGe layers has been studied previously using grazing-incidence white-beam topography,[8] but the lack of reciprocal-space resolution did not allow the contribution from each layer in the heterostructure to be imaged separately, as will be demonstrated here.

Figure 2 shows a high-resolution x-ray diffraction scan around the Si (004) Bragg peak from a 50 nm strained-Si film grown on a $Si_{0.8}Ge_{0.2}$ virtual substrate. The virtual substrate consists of a Si wafer, a 2-μm-thick $Si_{1-x}Ge_x$ linear

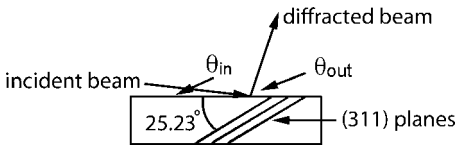

FIG. 1. A schematic of the grazing incidence diffraction geometry. The x-ray energy is selected so that the Bragg angle for the 311 planes is just larger than their inclination angle (25.23°) to the 001 surface, resulting in a grazing incident angle.

[a]Electronic mail: david.black@nist.gov

 © 2006 American Institute of Physics
Downloaded 22 May 2008 to 10.1.150.91. Redistribution subject to AIP license or copyright; see http://apl.aip.org/apl/copyright.jsp

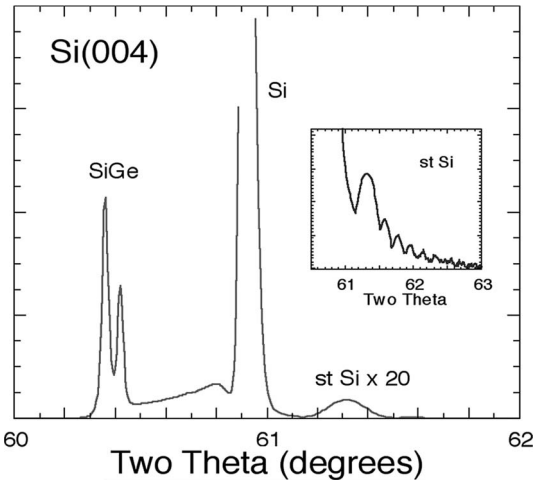

FIG. 2. High-resolution radial diffraction scan around the Si (004) Bragg condition for a 50 nm strained-Si/Si_xGe_{1-x}/Si(001) layered structure (linear scale). Clearly observed is diffraction from the Si wafer, the relaxed SiGe layer, and the resulting strained-Si film. The inset shows the diffraction from the strained-Si film on a log scale.

graded buffer layer where $x=0.0-0.2$, a 3-μm-thick constant-composition $Si_{0.8}Ge_{0.2}$ layer, and a 50 nm biaxially tensile strained-Si film. An *ex situ* planarization step was performed after 2.5 μm of the $Si_{0.8}Ge_{0.2}$ constant-composition layer had been grown, reducing its thickness to 1.7 μm. This planarization step is necessary to remove surface roughness and to prevent formation of dislocation pileups.[2] Thus the growth of the strained-Si film occurs after performing the *ex situ* planarization. Further details of wafer fabrication have been presented elsewhere.[3] The diffraction from the SiGe layers is seen near $2\theta=60.4°$; it appears as a doublet due to a slight compositional variation in the $Si_{0.8}Ge_{0.2}$ constant-composition layer grown before and after the *ex situ* planarization step. The sharp, intense peak near $2\theta=60.9°$ is diffraction from the Si wafer, and the much weaker peak near $2\theta=61.3°$ ($\times 20$ on this graph) is diffraction from the strained-Si film. (Note that the diffracted intensity from the Si wafer goes to infinity on this scale.) The strained-Si film has a smaller perpendicular lattice constant than the Si wafer, verifying that it is under in-plane tensile strain due to growth on the relaxed SiGe virtual substrate. The angular separation between the thick relaxed SiGe layer, the thin strained-Si film, and the Si wafer is due to the larger lattice constant of the SiGe and the Poisson ratio of Si. Kiessig interference fringes are visible in the inset log-scale plot of the strained-Si thin film, verifying the high crystalline quality of the film despite the presence of the defect structure and local strain fields (that result in the large mosaic width) that will be imaged below.

Figure 3 compares 311 asymmetric x-ray topographs from the layered structure of Fig. 2 recorded at the peaks of the Si wafer, the SiGe layer, and the strained-Si film. The strained-Si film could be found as a distinct peak only with an incident angle very near the critical angle. Energy and

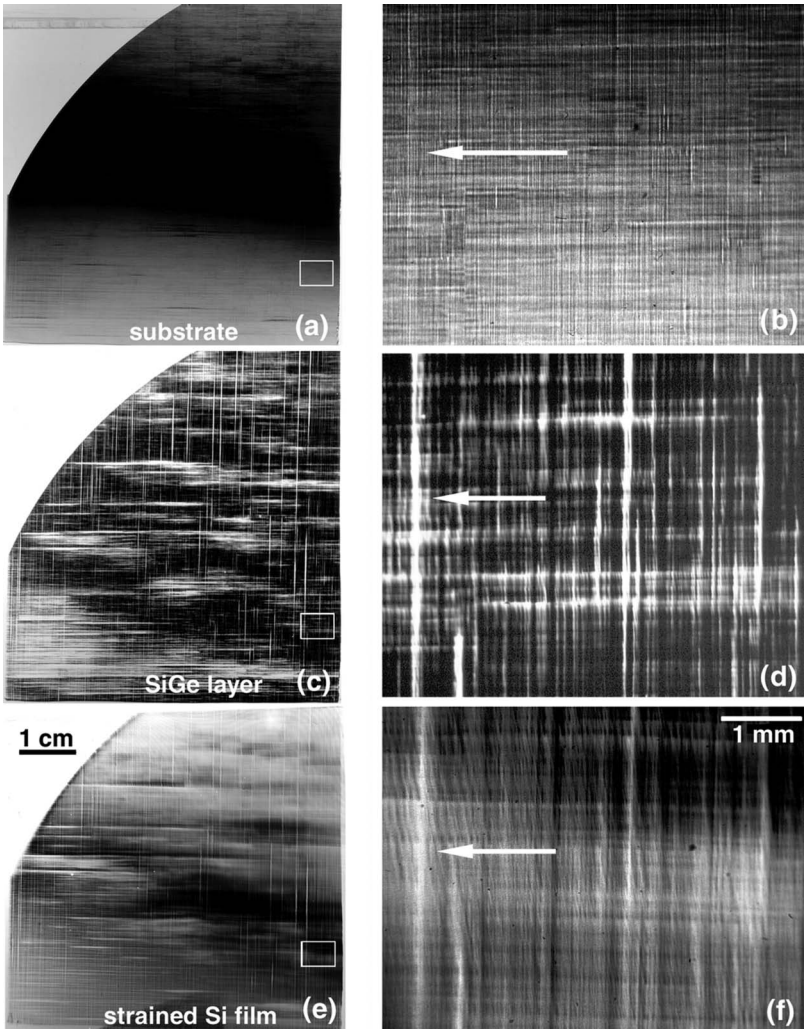

FIG. 3. Grazing-incidence (311) x-ray topographs at the peaks of [(a) and (b)] the Si wafer, [(c) and (d)] SiGe layer, and [(e) and (f)] strained-Si film from the strained-Si/Si_xGe_{1-x}/Si(001) layered structure of Fig. 1. These images were recorded at [(a) and (b)] $E=7.0$ keV, $\theta_{in}\sim 7.5°$, [(c) and (d)] $E=8.7$ keV, $\theta_{in}\sim 0.35°$, and [(e) and (f)] $E=9.0$ keV, $\theta_{in}\sim 0.25°$, respectively. At $E=8.9$ keV the critical angle is $\sim 0.2°$. The boxes in the lower magnification images [(a), (c), and (e)] identify the enlarged images on the right [(b), (d), and (f), respectively]. Note the nearly one-to-one correspondence of the defect structure in all three images.

Downloaded 22 May 2008 to 10.1.150.91. Redistribution subject to AIP license or copyright; see http://apl.aip.org/apl/copyright.jsp

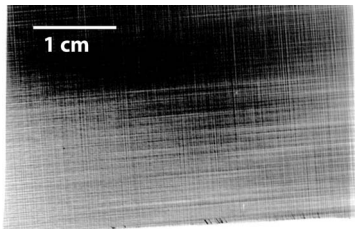

FIG. 4. A grazing-incidence (311) x-ray topograph of 45-nm-thick SSOI, $E=8.87$ keV, $\theta_{in}\sim 0.25°$. This image shows that the defect microstructure introduced from the misfit dislocations of the original SiGe layer persists after bonding the strained-Si donor wafer to the oxidized Si handle wafer and subsequent removal of the sacrificial SiGe virtual substrate. The Si substrate image (not shown) shows only the structure typical of a CMP-prepared silicon surface.

incident angles for each image are given in the figure captions. In all topographs, the projection of the diffraction vector is vertical in the image. The dislocation structure of the SiGe layer has the expected orthogonal crosshatch pattern oriented along the equivalent ⟨110⟩ directions. The microstructures of the strained-Si film and that of the SiGe layer are clearly related, demonstrating that the strain fields associated with the misfit dislocations responsible for the relaxation of the SiGe layer survive the planarization process and serve as a template for the microstructure of the strained-Si film. The topograph from the Si wafer demonstrates that the strain fields from the dislocations in the SiGe layer penetrate the silicon wafer surface, as there were no dislocations in the substrate wafer prior to growth. This image also confirms on a wafer scale the observation by cross-sectional transmission electron microscopy (TEM) of the injection into the wafer of threading segments of the misfit dislocations at the Si–SiGe interface.[9] These dislocations also result in broadened rocking curves (increased mosaic spread) as measured by x-ray diffraction (XRD) analysis.

Remarkably, once established by the underlying defect template, the microstructure of the strained-Si film remains even after the film is bonded to SiO_2 and separated from the SiGe virtual substrate to make strained-Si on insulator (SSOI). Figure 4 shows the microstructure of a 45-nm-thick strained-Si-on-insulator (SSOI) film; the SSOI substrate details have been presented elsewhere.[10] The defect structure in the SSOI film established by the original relaxed SiGe layer is visible, while the Si handle wafer image (not shown) shows only the typical structure that we observe from a chemomechanically polished (CMP) silicon surface. The SSOI has the same microstructure as strained Si, and it does not change even after heavy annealing to 1050 °C (image not shown). This image is consistent with, although on a much larger scale, the previous detection of misfit dislocations in supercritical (i.e., grown above the critical thickness) SSOI substrates by plan-view TEM.[10]

In conclusion, grazing-incidence x-ray topography has been used to image separately the defect structures in strained-Si films, their SiGe virtual substrates, and the base Si wafer of a 50 nm strained Si on SiGe-Si (001) layered structure. These images have shown that the dislocation structure of the SiGe layer acts as a template for the defect structure in the strained-Si film even after planarization, and it also penetrates the surface of the base Si wafer. Planarization removes surface roughness but not the residual strain fields at the surface from misfit dislocation structures formed at the interface. The microstructure of the strained-Si film remains intact, even when the film is removed from the SiGe virtual substrate, bonded to an oxidized wafer to make SSOI, and heavily annealed.

The UNICAT facility is supported by the U.S. DOE under Award No. DEFG02-91ER45439. The Advanced Photon Source is supported by the U.S. DOE, Basic Energy Sciences, Office of Science under Contract No. W-31-109-ENG-38.

[1] M. L. Lee, E. A. Fitzgerald, M. T. Bulsara, M. T. Currie, and A. Lochtefeld, J. Appl. Phys. **97**, 1 (2005).
[2] M. T. Currie, C. W. Leitz, T. A. Langdo, G. Taraschi, E. A. Fitzgerald, and D. A. Antoniadis, J. Vac. Sci. Technol. B **19**, 2268 (2001).
[3] J. G. Fiorenza, G. Braithwaite, C. W. Leitz, M. T. Currie, J. Yap, F. Singaporewala, V. K. Yang, T. A. Langdo, J. Carlin, M. Somerville, A. Lochtefeld, H. Badawi, and M. T. Bulsara, Semicond. Sci. Technol. **19**, L4 (2004).
[4] J. W. P. Hsu, E. A. Fitzgerald, Y. H. Xie, P. J. Silverman, and M. J. Cardillo, Appl. Phys. Lett. **61**, 1293 (1992).
[5] B. K. Tanner, *X-Ray Diffraction Topography* (Pergamon, Oxford, 1976).
[6] B. K. Bowen and B. Tanner, *High Resolution X-ray Diffractometry and Topography* (Taylor & Francis, London, 1998).
[7] D. R. Black and G. G. Long, NIST Report No. SP960-10, 2004.
[8] P. J. McNally, G. Dilliway, J. M. Bonar, A. Willoughby, T. Tuomi, R. Rantamäki, A. N. Danilewsky, and D. Lowney, Appl. Phys. Lett. **77**, 1644 (2000).
[9] K. W. Schwarz and F. K. LeGoues, Phys. Rev. Lett. **79**, 1877 (1997).
[10] T. A. Langdo, M. T. Currie, Z. Y. Cheng, J. G. Fiorenza, M. Erdtmann, G. Braithwaite, C. W. Leitz, C. J. Vineis, J. A. Carlin, A. Lochtefeld, M. T. Bulsara, I. Lauer, D. A. Antoniadis, and M. Somerville, Solid-State Electron. **48**, 1357 (2004).

Downloaded 22 May 2008 to 10.1.150.91. Redistribution subject to AIP license or copyright; see http://apl.aip.org/apl/copyright.jsp